Low-temperature dynamical simulation of spin-boson systems

Reinhold Egger* and C.H. Mak

Department of Chemistry, University of Southern California, Los Angeles, California 90089-0482

(Received 17 November 1993; revised manuscript received 1 June 1994)

The dynamics of spin-boson systems at very low temperatures has been studied using a real-time path-integral simulation technique, which combines a stochastic Monte Carlo sampling over the quantum fluctuations with an exact treatment of the quasiclassical degrees of freedom. To a large degree, this special technique circumvents the dynamical sign problem and allows the dynamics to be studied directly up to long real times in a numerically exact manner. This method has been applied to two important problems: (1) crossover from nonadiabatic to adiabatic behavior in electron-transfer reactions, (2) the zero-temperature dynamics in the antiferromagnetic Kondo region $\frac{1}{2} < K < 1$, where K is Kondo's parameter.

I. INTRODUCTION

Spin-boson systems provide archetypical models for many low-temperature dissipative quantum tunneling systems.[1-4] Applications include diverse problems such as the observability of macroscopic quantum coherence in a superconducting quantum interference device,[4] interstitial tunneling of light particles such as hydrogen in metals,[5] and many others discussed in Ref. 1. Two other examples are of special importance to this work. First, the so-called Kondo problem concerns localized spin impurities in nonmagnetic metals.[6] The second comes from the realm of chemical physics—in certain parameter regions, the spin-boson model provides a generalization of the Marcus model for electron-transfer reactions.[7-9] The wide range of applicability of the spin-boson model stems from its apparent generality—by coupling two exactly solvable models bilinearly, namely a two-state system (spin) and an infinite-dimensional harmonic oscillator (boson) bath, one obtains a nontrivial description for many dissipative systems.[10]

The dynamics of the spin-boson system has been widely studied using the Feynman-Vernon influence functional method,[11,12] mostly in conjunction with instanton techniques.[3] Much of the physics of this model has been unraveled by analytical methods, though an exact solution is not possible (except for some special parameter values). One particularly useful analytical approximation is the noninteracting blip approximation (NIBA).[3] Although the NIBA has been rather successful, there are important regions in parameter space where this approximation is expected to fail.

Very recently, numerical techniques for computing the dynamics of dissipative two-state systems have been developed.[13-16] These real-time quantum Monte Carlo (QMC) simulations have confirmed the NIBA predictions quantitatively in many cases, and in addition have provided information in regions where the NIBA breaks down. However, due to the fundamental *dynamical sign problem* inherent in these calculations,[17-22] the numeri-

cal computations are restricted in their accessible range of real times. The dynamical sign problem arises because at long times a large number of interfering paths contribute, leading to a very small signal-to-noise ratio. In effect, the simulation becomes unstable. Consequently, even numerically exact QMC methods have not been able to resolve many important questions concerning the behavior of the spin-boson system, especially at low temperatures and long times.

It is important to point out that many other approaches to dealing with the dynamical sign problem have been developed during the last decade. For example, methods based on related filtering techniques,[17,18] optimized reference systems,[19] or analytic continuation procedures following a conventional imaginary-time QMC simulation[20] have been proposed. Similar to the one described in this work, the first two methods attempt a direct simulation in real time. While we restrict our attention to *discrete* (tight-binding) systems which is adequate for many problems in low-temperature physics, most previous methods are designed for extended systems. On the other hand, the third method makes use of an imaginary-time simulation that has no dynamical sign problem to obtain numerical data which are then analytically continued to real times. To date, this procedure has only been used to find (e.g., electronic) spectral densities. While real-time information follows from the knowledge of these densities, such calculations have yet to be performed and hence the effectiveness of this approach to real-time dynamics is untested. We also point out that a similar numerical problem exists for QMC simulations of fermionic many-body systems.[23] This *fermion sign problem* has a different origin from the one dealt with here. It is due to the antisymmetry of fermionic wave functions, and makes even imaginary-time simulations problematic. If simulated in imaginary time, however, the spin-boson model does not pose any sign problem.

In this paper, we propose a simulation method to study the spin-boson dynamics numerically. Like our earlier approaches, this technique is based on a discretized path-

integral representation of the dynamical quantities of interest, but differs from them in that it exploits the symmetry properties of the influence functional. This allows for an exact treatment of the numerically problematic quasiclassical paths, and one is left with a stochastic Monte Carlo sampling of the quantum fluctuations alone. Related methods have been used previously to study quantum Brownian motion,[21,22] and we have used a similar algorithm to study the primary electron transfer steps in the bacterial photosynthetic reaction center.[24] Furthermore, this idea of exploiting the symmetries of the influence functional has also led to an efficient simulation method for computing the mobility and diffusion coefficient of a dissipative particle in an infinite tight-binding lattice.[25] The algorithm for this diffusion problem, however, is rather different from the one employed in the case of a system with a small number of tight-binding states. In this article, we provide a detailed description of our simulation method for the dissipative two-state system; the necessary generalizations for the case of more than two states should be obvious.

We apply this special method to the spin-boson model in the low-temperature and the small bath cutoff regions. The accuracy of the NIBA in some other parameter regions has been confirmed by our earlier simulations already, and the numerical results presented in this work focus on these previously inaccessible regions. Since the present algorithm is more powerful than previous methods, we are able to study longer times and much lower temperatures.

Data are presented for two practical problems of current interest: (1) electron transfer in a condensed phase environment, where we have examined the transition from nonadiabatic to adiabatic behavior for both the high-temperature and the low-temperature case. The high-temperature results should coincide with classical Marcus theory, whereas for low temperatures we would expect quantum effects commonly attributed to nuclear tunneling.[7] (2) The dissipative two-state system is also significant for the antiferromagnetic Kondo problem of a localized impurity embedded in a nonmagnetic metal.[6] The anisotropic Kondo Hamiltonian is related to the spin-boson model in a certain parameter region, and we have studied the most interesting antiferromagnetic case $1/2 < K < 1$, where K is Kondo's parameter, at zero temperature. An important question to be addressed in this parameter region relates to the destruction of quantum coherence. For $K < 1/2$, one can observe quantum coherence (oscillatory behavior) in the zero-temperature dynamics of the dissipative system. The NIBA predicts such coherent behavior to be completely destroyed for $K > 1/2$. Unfortunately, the justification for NIBA is suspect in this special parameter region, and our method offers a way of studying this region.

In Sec. II, we present our simulation method for the dissipative two-state system. The results for the crossover between nonadiabatic and adiabatic electron transfer are discussed in Sec. III, followed by a discussion of the dynamics in the antiferromagnetic Kondo region at very low temperatures. Some final remarks and conclusions are given in Sec. IV.

II. SIMULATION METHOD

In the following, we present a dynamical simulation technique for dissipative tight-binding models with a finite number of states. For simplicity, the discussion is restricted to the case of two states, which leads to the often-studied spin-boson Hamiltonian[3]

$$
\begin{aligned}
H &= H_0 + H_B + H_I \\
&= -(\hbar\Delta/2)\,\sigma_x + (\hbar\epsilon/2)\,\sigma_z \\
&\quad + \sum_\alpha \left[\frac{p_\alpha^2}{2m_\alpha} + \tfrac{1}{2}m_\alpha\omega_\alpha^2 \left(x_\alpha - \frac{C_\alpha}{m_\alpha\omega_\alpha^2}\sigma_z \right)^2 \right] \; . \quad (2.1)
\end{aligned}
$$

The parameters in the free Hamiltonian H_0 describing the isolated two-state system are the tunnel matrix element Δ—in the parlance of electron-transfer theory, $\Delta/2$ is the electronic coupling between the two different redox sites, the external bias ϵ corresponds to an asymmetry between the two localized energy levels, and σ_x and σ_z are the usual Pauli matrices. The bath is described by harmonic oscillators $\{x_\alpha\}$ which are bilinearly coupled to the spin operator σ_z. This type of coupling is reasonable for the problems considered in this work (and for many others); for a justification, see, e.g., Refs. 1–3.

Within this model, the bath parameters enter only via a single function called the spectral density

$$
J(\omega) = \frac{\pi}{2} \sum_\alpha \frac{C_\alpha^2}{m_\alpha\omega_\alpha} \delta(\omega - \omega_\alpha) \, , \quad (2.2)
$$

which should have a continuous form in the limit of infinitely many bath oscillators. The spectral density then determines the bath correlation function[9]

$$
L(z) = \frac{a^2}{\pi\hbar} \int_0^\infty d\omega \, J(\omega) \frac{\cosh[\omega(\hbar\beta/2 - iz)]}{\sinh[\omega\hbar\beta/2]} \, , \quad (2.3)
$$

which is defined for complex-valued times $z = t - i\tau$. The distance between the localized states is given by a length scale a, and $\beta = 1/k_B T$. Here, we limit our attention to the case of an Ohmic spectral density which has the form

$$
J(\omega) = (2\pi\hbar K/a^2)\,\omega\, e^{-\omega/\omega_c} \, . \quad (2.4)
$$

This spectral density has a characteristic low-frequency behavior $J(\omega) \sim \eta\omega$, where η is the usual Ohmic viscosity. The system-bath coupling strength is measured in terms of the dimensionless Kondo parameter K. The time scale distribution of bath motions is described by a cutoff frequency ω_c. For many problems in low-temperature physics, this cutoff frequency is taken to be the largest frequency scale in the problem. In the case of electron transfer, the same spectral density with some intermediate value for ω_c is most appropriate for a realistic description of many polar solvents.[26]

Two dynamical quantities of interest for this model are the symmetrized time correlation function

$$
\begin{aligned}
C(t) &= \mathrm{Re}\,\langle \sigma_z(0)\sigma_z(t) \rangle \\
&= Z^{-1}\mathrm{Re}\,\mathrm{Tr}\left(e^{-\beta H}\sigma_z e^{iHt/\hbar}\sigma_z e^{-iHt/\hbar} \right) \quad (2.5)
\end{aligned}
$$

with $Z = \text{Tr}\, e^{-\beta H}$, and the time-dependent occupation probabilities for the two sites $P_+(t)$ and $P_-(t)$ which can be expressed in terms of a single function

$$P(t) = P_+(t) - P_-(t) = \langle e^{iHt/\hbar}\sigma_z e^{-iHt/\hbar}\rangle \qquad (2.6)$$

with the initial condition $P(0) = 1$. From a comparison of Eqs. (2.5) and (2.6) we observe that the two quantities differ only by the way the system is prepared initially. For $P(t)$, the system is held fixed in the $+$ state until $t = 0$ with the bath being unobserved (factorized initial condition). On the other hand, the more realistic situation for many experiments is represented by equilibrium states of the total system at $t = 0$ as described by $C(t)$.

To numerically compute the two-state dynamics, we employ a discretized path-integral representation of the dynamical quantities.[12-15] The correlation function $\langle\sigma_z(0)\sigma_z(t)\rangle$ can be regarded as the probability amplitude for a sequence of steps in the complex-time plane. In particular, one propagates along the Kadanoff-Baym contour γ: $z = 0 \to t \to 0 \to -i\hbar\beta$, and measures σ_z at $z = 0$ and $z = t$. Of course, there are several other possible choices of this contour due to the cyclic structure of the trace.

To parametrize the paths, we use q uniformly spaced discrete points for each of the two real-time paths and r points for the imaginary-time path (see Fig. 1). Hence, there are $N = 2q + r$ points in total. The time discretizations are

$$\Delta_j = \begin{cases} t/q, & 1 \le j \le q \\ -t/q, & q+1 \le j \le 2q \\ -i\hbar\beta/r, & 2q+1 \le j \le 2q+r \equiv N \end{cases} \qquad (2.7)$$

and the complex time after i steps is $z_i = \sum_{j=1}^{i-1}\Delta_j$. The construction of the discretized path integral then proceeds by inserting complete sets

$$1_i = \sum_{\sigma_i = \pm 1}\int\prod_\alpha dx_{\alpha,i}\,|\sigma_i,\{x_{\alpha,i}\}\rangle\langle\sigma_i,\{x_{\alpha,i}\}|$$
$$= \int d\mathbf{r}_i\,|\mathbf{r}_i\rangle\langle\mathbf{r}_i| \qquad (2.8)$$

at each discretization point z_i $(i = 2, \ldots, N)$. The vector $\mathbf{r}_i$ represents the state $\sigma_i = \pm 1$ of the two-level system as well as the environmental degrees of freedom $\{x_{\alpha,i}\}$.
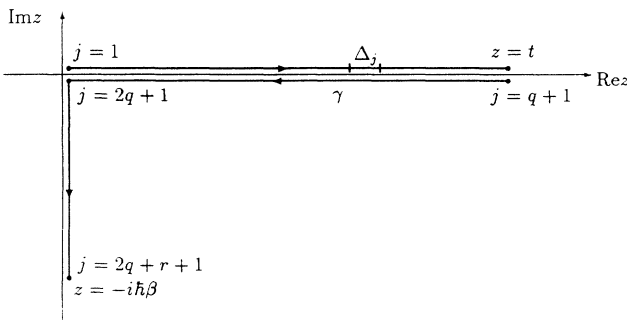

FIG. 1. Discretization of the Kadanoff-Baym contour γ in the complex-time plane.

To disentangle the short-time propagator, we use a (symmetrized) Trotter formula,

$$\exp(-iH\Delta_j/\hbar) = \exp(-iH'\Delta_j/2\hbar)\exp(-iH_0\Delta_j/\hbar)$$
$$\times \exp(-iH'\Delta_j/2\hbar) + O(\Delta_j^3[H_0,H']), \qquad (2.9)$$

where $H' = H - H_0$ is diagonal in the representation (2.8). The free part H_0 of the Hamiltonian (2.1) leads to the short-time propagator

$$K(\sigma_j,\sigma_{j+1}) = \langle\sigma_{j+1}|\exp(-i\Delta_j H_0/\hbar)|\sigma_j\rangle \qquad (2.10)$$

which can be evaluated exactly. Thereby we arrive at

$$\langle\sigma_z(0)\sigma_z(t')\rangle = \frac{\int d^N\mathbf{r}\,e^{S[\mathbf{r}_1,\ldots,\mathbf{r}_N]}\sigma'\sigma''}{\int d^N\mathbf{r}\,e^{S[\mathbf{r}_1,\ldots,\mathbf{r}_N]}}, \qquad (2.11)$$

which converges to the true path integral as the number of discretizations $N \to \infty$. The discretized action $S[\mathbf{r}_1,\ldots,\mathbf{r}_N]$ is a complex-valued sum of the actions picked up in separate parts of the contour γ. To compute the correlation function in Eq. (2.11), one can average over all pairs of spins $\{\sigma',\sigma''\}$ separated by a time t' along the contour γ. This allows us to compute the dynamical quantities for all times $t_k = kt/q$ (where $k = 0,\ldots,q$) from one single Metropolis trajectory. Because of the cyclic structure of the trace in Eq. (2.5), $\mathbf{r}_{N+1} \equiv \mathbf{r}_1$.

Since the bath is made up of harmonic oscillators, one can integrate out the environmental degrees of freedom analytically. After performing this integration, the bath-plus-coupling part H' of the Hamiltonian leads to an *influence functional* $\Phi[\sigma]$ in terms of the spins $\{\sigma_i\}$ alone.[11,12] As a result, the correlation function takes the form

$$\langle\sigma_z(0)\sigma_z(t')\rangle = \frac{1}{Z}\sum_{\{\sigma\}}\exp\left(-\Phi[\sigma] + \sum_i \ln K(\sigma_i,\sigma_{i+1})\right)\sigma'\sigma'', \qquad (2.12)$$

where $Z = \sum_{\{\sigma\}}\exp(\ldots)$ (the exponent will be referred to as "the action" henceforth). In the continuum limit $N \to \infty$, the nonlocal influence functional is given in terms of the bath correlation function $L(z)$ introduced in Eq. (2.3), and one finds with $\sigma_i \to \sigma(z)$ Ref. 27

$$\Phi[\sigma] = \int_\gamma dz\int_{z'<z}dz'\,\sigma(z)L(z-z')\sigma(z')/4. \qquad (2.13)$$

The integrations in the complex-time plane are ordered along the Kadanoff-Baym contour γ. Note that $L(z)$ fulfills the important symmetry relation

$$L(z - i\hbar\beta) = L(-z), \qquad (2.14)$$

which implies certain symmetry properties of the influence functional.

In discretized form, the influence functional is given by[12]

$$\Phi[\sigma] = \tfrac{1}{2} \sum_{j,k=1}^{N} \sigma_j L_{jk} \sigma_k / 4 \,, \qquad (2.15)$$

with the complex-valued influence matrix L_{jk}. We observe from Eqs. (2.12) and (2.15) that the (discretized) spin-boson problem is isomorphic to a classical one-dimensional Ising model with long-range complex-valued interactions.[12,13] The influence matrix is the average value of the influence functional interaction between two points z_j and z_k

$$L_{jk} = L_{kj} = \int_{C_j} dz'_j \int_{C_k} dz'_k \, L(z'_j - z'_k) \qquad \text{for } j > k \,, \qquad (2.16)$$

where C_i is one discretization on the contour centered at the point z_i, i.e.,

$$\{z \in C_i | z_i - \Delta_{i-1}/2 < z < z_i + \Delta_i/2\} \,.$$

The remaining time integrations in Eq. (2.16) can be carried out easily, and one finds with $\Delta_{jk} = z_j - z_k$

$$\begin{aligned} L_{jk} = &\, Q(\Delta_{jk} + (\Delta_j + \Delta_{k-1})/2) \\ &+ Q(\Delta_{jk} + (-\Delta_{j-1} - \Delta_k)/2) \\ &- Q(\Delta_{jk} + (-\Delta_{j-1} + \Delta_{k-1})/2) \\ &- Q(\Delta_{jk} + (\Delta_j - \Delta_k)/2) \,, \end{aligned} \qquad (2.17)$$

where $Q(z)$ is the twice-integrated bath correlation function with $Q(0) = 0$, i.e., $d^2Q(z)/dz^2 = L(z)$. Of course, this function exhibits the same symmetry property (2.14). Finally, the diagonal elements are given by

$$L_{jj} = 2Q((\Delta_{j-1} + \Delta_j)/2) \,.$$

A detailed derivation of the influence matrix can be found in Refs. 15 and 24.

Since the action for each spin configuration (a path) is complex valued, a stochastic Monte Carlo evaluation of the resulting isomorphic Ising chain is faced with the dynamical sign problem. In the past, we have partially circumvented this problem either by transforming to a continuous spin representation and applying stationary-phase Monte Carlo (SPMC) methods,[13,15] or by introducing a local filtering function in discrete state space.[14,16] The latter approach is related to ideas like the stationary-phase approximation and allowed for a study of many phenomena on an intermediate time scale.

Here, we observe that a much more efficient method can be constructed when one takes into account the symmetry properties of the influence matrix due to Eq. (2.14). These symmetry relations can be expressed mathematically as a set of index relations (we use $i, j, k = 1, \ldots, q+1$, and $n, m = 2, \ldots, r$)

$$L_{2q+2-i,2q+2-j} = L^*_{ij}, \quad L_{2q+2-i,j} = -L^*_{ij} \text{ for } j > i, \quad L_{2q+2-i,j} = -L_{ij} \text{ for } i > j \,,$$

$$L_{2q+2-i,i} = -\text{Re}\,L_{ii}, \quad L_{2q+m,2q+2-j} = -L_{2q+m,j} \text{ for } j > 1, \quad L_{i,q+1} = L_{2q+2-i,q+1} = L_{2q+m,q+1} = 0 \,,$$

which can be proved easily from Eq. (2.17).

The benefit of exploiting these relations is realized upon switching to a new spin representation. To that purpose, we introduce the sum and difference coordinates of the forward (σ_j) and backward (σ'_j) real-time spin paths and rename the imaginary-time spins ($\bar{\sigma}_m$),

$$\eta_j = (\sigma_j + \sigma'_j)/2,$$
$$\xi_j = (\sigma_j - \sigma'_j)/2, \qquad (2.18)$$
$$\bar{\sigma}_m = \sigma_{2q+m} \,,$$

where $\sigma'_j = \sigma_{2q+2-j}$ in the old notation ($j = 1, \ldots, q+1$). Thus we first relabel the spins on the three pieces of the Kadanoff-Baym contour and then form the said linear combinations. A physical meaning can be assigned to these new spins: $\{\eta_j\}$ describe the propagation along the diagonal of the reduced density matrix and can thus be identified with *quasiclassical paths*, while $\{\xi_j\}$ describe the off diagonaliticity of the reduced density matrix and can be identified with *quantum fluctuations*.[28] According to the definitions (2.18), the new spins can take on three possible values $\xi, \eta = -1, 0, 1$, but they are not entirely independent because either ξ_j or η_j has to be 0 for the same j.

Written in terms of the new spins and exploiting the index relations above, the influence functional takes the form

$$\begin{aligned} \Phi[\xi, \eta, \bar{\sigma}] = &\, \tfrac{1}{2} \sum_{m,n=2}^{r} \bar{\sigma}_m Y_{mn} \bar{\sigma}_n + \tfrac{1}{2} \sum_{j,k=1}^{q} \xi_j \Lambda_{jk} \xi_k \\ &+ i \sum_{j>k=1}^{q} \xi_j X_{jk} \eta_k + \sum_{j=1}^{q} \sum_{m=2}^{r} \xi_j Z_{jm} \bar{\sigma}_m \\ &+ \eta_1 \left(\sum_{m=2}^{r} \bar{\sigma}_m \left[L_{2q+m,1} + L_{2q+m,2q+1} \right] \right) \,. \end{aligned} \qquad (2.19)$$

The elements of the matrices appearing in Eq. (2.19) are

$$Y_{mn} = L_{2q+m,2q+n}/4 \,,$$
$$\Lambda_{jk} = \text{Re}\,L_{jk} \,,$$
$$X_{jk} = \text{Im}\,L_{jk} \,,$$
$$Z_{jm} = L_{j,2q+m}/2 \,.$$

It is worth mentioning that these matrices are *real valued* (with the exception of Z_{jm}). The meaning of the five terms in Eq. (2.19) is as follows. The first term describes a self-interaction within the imaginary-time segment. Due to the second term, the dissipative bath will damp out the quantum fluctuations, and the system is likely to be found in a diagonal state characterized by $\xi = 0$. This point will later be important with regard to the choice of a suitable Monte Carlo weight. The third term is a bilinear interaction between quasiclassical paths

and quantum fluctuations, and the fourth term describes a similar interaction between the imaginary-time spins and the quantum fluctuations. The last term is a preparation term, coupling η_1 to the imaginary-time spins. Remarkably, there is no self-interaction in the quasiclassical paths, and they are coupled only linearly to other degrees of freedom.

This observation is crucial for our computational procedure, since it allows for an exact treatment of the quasiclassical paths. *For any given quantum fluctuation path, the path summation over all allowed quasiclassical paths can be carried out in an exact manner.* To elucidate this, we first examine the free action due to H_0. The imaginary-time contribution can be put into the matrix elements Y_{mn} by simply adding $\frac{1}{2}\ln\tanh(\hbar\beta\Delta/2r)$ to $Y_{m,m+1}$ and $Y_{m+1,m}$; in case an external bias ϵ is present, the action has to include an additional term $(\hbar\beta\epsilon/2r)\sum_m \bar{\sigma}_m$.[15] Regarding the real-time paths, we proceed in a different way. For the isolated two-state system, we have (in terms of the original spins) a product of the form [cf. Eq. (2.10)]

$$\prod_{j=1}^{q} K(\sigma_j, \sigma_{j+1}) K^*(\sigma_j', \sigma_{j+1}') \ . \tag{2.20}$$

If we now switch to the $\{\xi, \eta\}$ representation and perform the summation over all η spins (while keeping the ξ configuration frozen), we obtain a *matrix product* for Eq. (2.20). Of course, one has to account for the η-dependent terms in the influence functional (2.19) during this procedure. In the end, the complex-valued contribution of all these terms for a given ξ configuration takes the form

$$J[\xi] = \sum_{\eta_1=0,\pm1} \sum_{\eta_{q+1}=0,\pm1} \langle \eta_1 | \mathbf{V}^{(1)} \ldots \mathbf{V}^{(q)} | \eta_{q+1} \rangle \ , \quad (2.21)$$

where the (3×3) matrices $\mathbf{V}^{(j)}[\xi]$ are defined by[29]

$$\langle \eta_j | \mathbf{V}^{(j)} | \eta_{j+1} \rangle = [K \times K^*](\eta_j, \eta_{j+1}, \xi_j, \xi_{j+1})$$

$$\times \exp\left[-i\eta_j \sum_{k>j}^{q} X_{kj}\xi_k \right] \ . \tag{2.22}$$

Each of the matrices $\mathbf{V}^{(j)}$ depends on all ξ_k spins with $k \geq j$; however, the "free" part $K \times K^*$ is determined by ξ_j and ξ_{j+1} alone. Clearly, $J[\xi]$ can be evaluated with a simple matrix multiplication routine, leading to a numerically exact and efficient treatment of the quasiclassical paths. Note that the remaining part of the influence functional is real-valued — with the exception of the fourth term in Eq. (2.19), which is generally very small — indicating that much of the dynamical sign problem has been relieved by treating the numerically problematic quasiclassical paths in an exact manner.

In effect, the factor $J[\xi]$ contains all contributions from H_0 and, in addition, the third and fifth term of the influence functional (2.19). The correlation function can thus be written as

$$\langle \sigma_z(0)\sigma_z(t') \rangle = \frac{1}{Z} \sum_{\{\xi\}=-1,0,1} \sum_{\{\bar{\sigma}\}=\pm1} J[\xi]$$

$$\times \exp\left(-\frac{1}{2} \sum_{m,n=2}^{r} \bar{\sigma}_m Y_{mn} \bar{\sigma}_n \right.$$

$$-\frac{1}{2} \sum_{j,k=1}^{q} \xi_j \Lambda_{jk} \xi_k$$

$$\left. - \sum_{j=1}^{q} \sum_{m=2}^{r} \xi_j Z_{jm} \bar{\sigma}_m \right) \sigma' \sigma'' \ .$$

Therefore, we are left with the task of summing over the imaginary-time spins $\{\bar{\sigma}_m\}$ and the quantum fluctuations $\{\xi_j\}$, which is conveniently done via Monte Carlo (MC) sampling. The suitable MC weight for the imaginary-time spins is straightforward,

$$P_{\text{imag}}[\bar{\sigma}] \sim \exp\left(-\frac{1}{2} \sum_{m,n} \bar{\sigma}_m Y_{mn} \bar{\sigma}_n - \text{Re} \sum_{j,m} \xi_j Z_{jm} \bar{\sigma}_m \right) \ .$$

Since the influence functional forces the quantum fluctuations to stay near the diagonal of the density matrix, we first try to use the following MC weight for the quantum fluctuations

$$P_{\text{real}}[\xi] \sim \exp\left(-\frac{1}{2} \sum_{j,k} \xi_j \Lambda_{jk} \xi_k - \text{Re} \sum_{j,m} \xi_j Z_{jm} \bar{\sigma}_m \right) \ .$$

The problem with this weight, however, arises for small system-bath couplings where the damping of the quantum fluctuations becomes weak. In this case, the importance sampling would become very inefficient for small coupling K. Hence, in a next step, we try the product

$$W[\xi] \sim P_{\text{real}}[\xi] \times |J[\xi]| \ ,$$

where $J[\xi]$ has been defined in Eq. (2.21). This weight function considers both the damping of the quantum fluctuations due to the influence functional *and* the integrated-out quasiclassical paths.

Unfortunately, there is another problem with this weight, similar to the case of the multistate algorithm.[25,30] This problem arises since for correlation functions such as $\langle \sigma_z(0)\sigma_z(t) \rangle$ one has to compute the ratio of two quantities. It turns out that certain spin configurations only contribute to the denominator but not to the numerator (and vice versa). Due to this exclusivity problem, one will not be able to access all relevant spin configurations $\{\xi\}$ contributing to the numerator when using $W[\xi]$ alone as the Monte Carlo weight. We can circumvent this problem by observing that for the numerator, one has to compute terms such as [where $\alpha_1, \alpha_2 = \pm$]

$$J_{\alpha_1,\alpha_2}^{(k)}[\xi] = \sum_{\eta_1=0,\pm1} \sum_{\eta_{q+1}=0,\pm1} \langle \eta_1 | H_{\alpha_1}$$

$$\times (\xi_1) \mathbf{V}^{(1)} \ldots \mathbf{V}^{(k-1)} H_{\alpha_2}$$

$$\times (\xi_k) \mathbf{V}^{(k)} \ldots \mathbf{V}^{(q)} | \eta_{q+1} \rangle \ . \tag{2.23}$$

The projection operators $H_+ = (1+\sigma_z)/2$ and $H_- = (1-\sigma_z)/2$ onto the two spin values have the η representation (for a given ξ)

$$H_+(\xi = 0) = \begin{pmatrix} 1 & 0 & 0 \\ 0 & 0 & 0 \\ 0 & 0 & 0 \end{pmatrix}, \quad H_-(\xi = 0) = \begin{pmatrix} 0 & 0 & 0 \\ 0 & 0 & 0 \\ 0 & 0 & 1 \end{pmatrix},$$

$$H_\pm(\xi = \pm 1) = \begin{pmatrix} 0 & 0 & 0 \\ 0 & 1/2 & 0 \\ 0 & 0 & 0 \end{pmatrix}.$$

Finally, an appropriate positive definite Monte Carlo weight function can be constructed

$$\widetilde{W}[\xi] \sim P_{\text{real}}[\xi] \left(\sum_{k=1}^{q} \sum_{\alpha_1,\alpha_2=\pm} \left| J_{\alpha_1,\alpha_2}^{(k)} \right| \right). \tag{2.24}$$

Using $\widetilde{W}[\xi]$ as the weight allows us to carry out an efficient Monte Carlo sampling of the ξ spins.

Our QMC algorithm employs single-particle Metropolis moves as well as moves that allow kinks to translate along the spin chain.[16] Single-particle moves attempt to change one spin $\xi_k = -1, 0, 1$ to a new value, whereas kink moves attempt to change two adjacent spins simultaneously. The imaginary-time spins are sampled from $P_{\text{imag}}[\bar{\sigma}]$ using single-particle moves, i.e., one tries to flip a single spin $\bar{\sigma}_m = \pm 1$. During one MC pass, the single-particle moves are attempted once for every spin, and the kink moves are attempted for every pair of spins with $\xi_k \neq \xi_{k+1}$. Typical acceptance ratios for these types of moves are $\approx 15\%$, and we take samples separated by 5 MC passes. This ensures that the MC samples are sufficiently uncorrelated, since roughly half of the spins have been assigned new values between two subsequent samples. Numerical results are then obtained from several 10 000 samples, with statistical errors always below 5% for the data reported here.

The calculations were carried out on an IBM RISC 6000/580 workstation, at an average speed of 2 CPU hours per 10 000 samples (for $q \approx 80, r = 0$). As mentioned earlier, the dynamical quantities of interest can be sampled from a single Monte Carlo trajectory for all times $t' \leq t$ since the remaining part of the Kadanoff-Baym contour can be integrated out. Furthermore, the quantity $P(t)$ can be calculated using the same code by simply removing all spins from the imaginary-time path, i.e., by putting $r = 0$. Finally, to ensure that the Trotter error is sufficiently small, we have to keep the discretization numbers q and r large enough. This is checked by systematically increasing these numbers until convergence is reached. For all results presented here, the Trotter error is negligible compared to the statistical errors due to the stochastic MC sampling (which are less than 5%).

We close this section with some remarks concerning the relation between this method and our earlier techniques. The algorithm presented here can be thought of as an optimized (but essentially nonlocal) filtering method for discrete-state systems as proposed by Mak.[14] The optimization is achieved by exploiting the underlying symme-

TABLE I. Performance of different dynamical simulation techniques for spin-boson systems: (a) a brute-force evaluation of the path integrals without any filtering, (b) the SPMC calculation (Refs. 13,15), (c) the original discrete filtering technique (Refs. 14,16), (d) the current optimized filtering method. The data shown below are for a calculation of $P(t)$ for $K = 1/2, \omega_c/\Delta = 6$, both for $T = 0$ and for a high temperature, $\Delta\beta = 0.5$. For times $t > t_{\text{max}}$, the dynamical sign problem becomes uncontrollable (with statistical errors > 20%).

	Δt_{max} for $\beta\Delta = \infty$	Δt_{max} for $\beta\Delta = 0.5$
(a)	5	8
(b)	9	14
(c)	12	18
(d)	22	24

tries of the influence functional. This makes this method superior in the sense that we can study longer times with less computational effort. Since the dynamical sign problem grows exponentially with increasing time, most of the results discussed in the next section cannot be obtained by any former technique. An approximate measure for the performance of the different real-time QMC algorithms for the spin-boson problem can be obtained from the maximum real time t_{max} defined as the upper time limit of the respective method. For times $t > t_{\text{max}}$, the large statistical errors caused by the dynamical sign problem (more than $\approx 20\%$) will render the simulation results useless. This is quantified in Table I. The comparison with earlier methods demonstrates that the spin-boson dynamics can now be studied up to much longer time scales despite the dynamical sign problem. The gain is most significant at very low temperatures, but is also important at higher temperatures.

III. SIMULATION RESULTS

In this section, we present dynamical simulation results for two different problems, namely the crossover between nonadiabatic and adiabatic electron transfer and the dynamics in the low-temperature antiferromagnetic Kondo region. We will restrict our attention to the symmetric case $\epsilon = 0$ here, and we also consider only Ohmic spectral densities of the form (2.4). For numerical results in other parameter regions of the spin-boson model, we refer to our previous work.[13-16]

A. Crossover from nonadiabatic to adiabatic electron transfer

The spin-boson system is an adequate model for many electron transfer reactions in condensed phase systems.[9] The electron-transfer rate is, in general, determined not only by the overlap of the electronic wave functions localized on the redox states (which is proportional to the tunnel splitting Δ), but also by the properties of the solvent environment. For a charge transfer to occur, a specific

large-scale reorganization of the solvent is required to achieve the resonance condition necessary for electronic tunneling. Using linear response theory for a description of the solvent modes and a tight-binding model for the redox states, one arrives at the spin-boson model. In our study, we have taken an Ohmic spectral density (2.4) for the bath with a finite cutoff frequency ω_c which can be regarded as a free parameter.[26]

The solvent is described by a continuous spectral density peaked around a characteristic bath mode frequency ω_c, and the classical reorganization energy corresponding to this bath is $\hbar\lambda = 2K\hbar\omega_c$, where K is Kondo's parameter. For typical electron-transfer reactions, the reorganization energy fulfills the condition $\lambda/\Delta \gg 1$. The nonadiabatic regime of electron-transfer is defined by small electronic couplings, $\Delta/\omega_c \ll 1$, whereas the adiabatic limit corresponds to electronic couplings of the order of ω_c (or larger). We note that the nonadiabatic limit is realized in most biological and in many chemical systems; nevertheless, the adiabatic limit is also important for a description of many chemical electron-transfer reactions.

The high-temperature limit of electron transfer is well understood within the framework of classical Marcus and Sutin theory.[7] The rate can be factored into an equilibrium Boltzmann factor containing the activation free energy for the required global bath fluctuation, and a Landau-Zener factor for the transition probability once this Landau-Zener region has been reached.[8] For symmetric electron-transfer reactions, Marcus found a bath activation energy $\hbar\lambda/4$, and combining this with a conventional estimate for the Landau-Zener factor,[8] one obtains a formula for the total (forward plus backward) rate[31]

$$\Gamma = \sqrt{\frac{\pi\hbar\beta}{4\lambda}} \frac{\Delta^2}{1 + \Delta^2/\omega_b\lambda} \exp(-\beta\hbar\lambda/4) , \qquad (3.1)$$

which is valid for $\hbar\beta\omega_c \ll 1$. The Landau-Zener factor contains a frequency scale ω_b reminiscent of transition state theory which is usually applied to the adiabatic limit.[9] Note that for small electronic couplings, the rate $\sim \Delta^2$ which is just the golden rule behavior. In the adiabatic limit of large Δ, however, the rate becomes independent of Δ, and the dynamics is totally solvent controlled. We note that for the spectral density (2.4), one can obtain analytical expressions in the nonadiabatic golden rule limit for both the high- and low-temperature rate ($T' = \hbar\omega_c/k_B$ provides a rough measure for the temperature below which quantum effects due to nuclear tunneling become important). For the special values $K = 1/2$ and $K = 1$, the crossover behavior from high to low temperatures can be solved explicitly.[26]

In Fig. 2 we show some results for $P(t)$ in the high-temperature limit; in this parameter region, the effects of the initial preparation are negligible, so $C(t) = P(t)$. For a study of the crossover between nonadiabatic and adiabatic behaviors, all model parameters except Δ are kept fixed. In the case of small Δ, the simulation results exhibit a monoexponential decay on the golden rule time scale. However, for larger Δ, the dynamics becomes progressively more complex. After a fast initial tran-
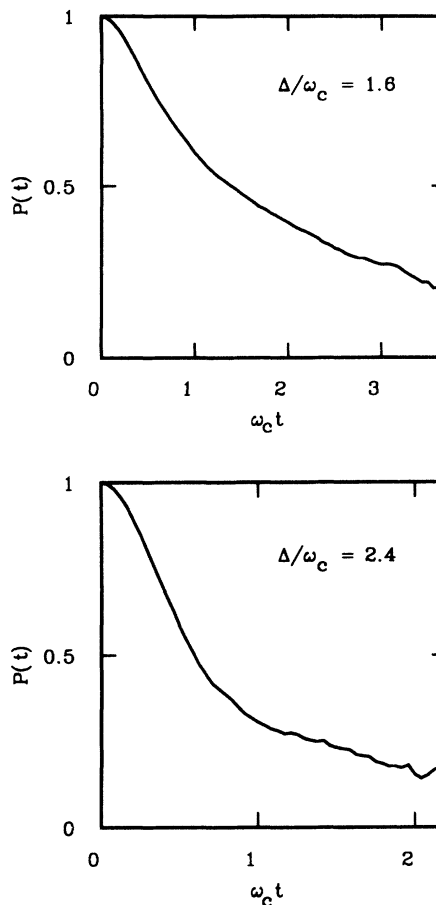

FIG. 2. Simulation results for $K = 2$, $k_B T/\hbar\omega_c = 4$ and two values of the electronic coupling. Note the change in time scale.

sient, the decay slows down; fitting this slower decay to an exponential law, one can again extract a rate for this adiabatic situation.

The Δ-dependent high-temperature rates measured in units of ω_c are plotted in Fig. 3. Clearly, the nonadiabatic limit is nicely reproduced by the simulations for small Δ, and the rates $\sim \Delta^2$. In the adiabatic limit, the rate constant is approximately *independent* of the magnitude of the electronic coupling. These results are in agreement with the conventional Landau-Zener prediction (3.1) in the limit of high temperatures. Remarkably, the data in Fig. 3 show that the golden rule formula is accurate for values of Δ/ω_c as large as ≈ 1.5. Note also that we find a monotonic dependence of the rate on Δ, in contrast to the findings of Skourtis et al.[32] which are based on a rather simplistic Hamiltonian and would predict a maximum in the rate as a function of Δ.

Next we study the low-temperature region ($\hbar\beta\omega_c = 2.5$), where the classical rate formula (3.1) is not expected to hold. Again, we find complete agreement with the nonadiabatic golden rule formalism for small values of Δ/ω_c, with $P(t)$ decaying monoexponentially on the golden rule time scale (with a fast initial transient). When increasing Δ/ω_c beyond ≈ 0.5, however,
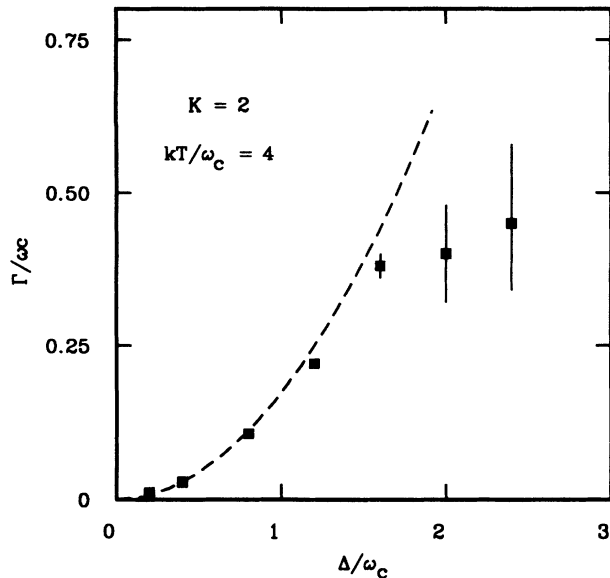
FIG. 3. Electron-transfer rate constants as a function of the electronic coupling; squares denote decay constants of $P(t)$ for $K = 2$, $k_BT/\hbar\omega_c = 4$, i.e., total rates. The dashed line is the nonadiabatic golden rule prediction, and vertical bars are error estimates.
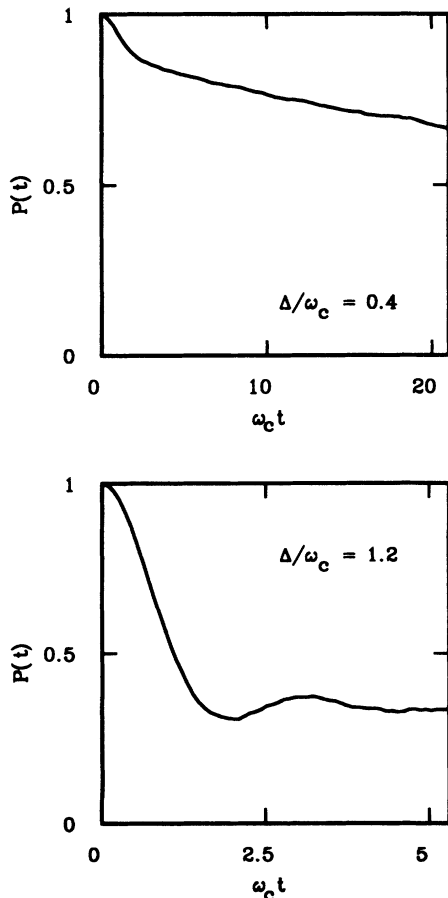
FIG. 4. Simulation results for $K = 2$, $k_BT/\hbar\omega_c = 0.4$ and two values of the electronic coupling. Note the change in time scale.

the dynamics exhibits an oscillatory behavior as shown in Fig. 4. This prevents a meaningful estimate for the decay constant (but when increasing K to significantly larger values, we expect that the dynamics will become totally incoherent again, at least for not too small ω_c/Δ). We note that in the limit $\omega_c/\Delta \to 0$ (but λ finite), the dynamics can be solved exactly. This is the case of a strictly adiabatic bath,[9] where the dynamics is always oscillatory. From the simulations we also observe that the nonadiabatic regime is confined to increasingly smaller values for Δ/ω_c when the temperature is lowered.

In conclusion, the simulations confirm the classical picture for the crossover from nonadiabatic to adiabatic electron transfer in the high-temperature limit and, in addition, provide a dynamical explanation. In the low-temperature limit, however, the dynamics becomes oscillatory unless the system-bath coupling is made very large.

B. Antiferromagnetic Kondo region: low-temperature dynamics

We next turn to a different problem. The determination of the dynamical quantities of interest in the low-temperature Kondo region characterized by a Kondo parameter $1/2 < K < 1$ has been a long-standing problem.

We start with a brief discussion of the relationship of the spin-boson model to the Kondo problem.[6] The Kondo Hamiltonian in its simplest form describes a spin-$\frac{1}{2}$ impurity interacting with a band of free electrons via isotropic exchange scattering. A particularly useful method for studying the low-temperature spin relaxation dynamics of the Kondo problem (the equilibrium properties are well understood[6]) employs a bosonization procedure to map it onto a spin-boson problem with Ohmic dissipation.[3] The case $1/2 < K < 1$ then corresponds to the interesting antiferromagnetic Kondo problem. The important dynamical quantity in the Kondo problem is the imaginary part of the frequency-dependent spin susceptibility $\chi''(\omega)$. It can be expressed in terms of the Fourier transform of the correlation function (2.5)

$$C(\omega) = \hbar\coth(\beta\hbar\omega/2)\chi''(\omega) .$$ (3.2)

Therefore, a computation of $C(t)$ will yield all relevant dynamical quantities (structure factor, dynamical susceptibility, etc.) of the Kondo problem.

Unfortunately, the noninteracting blip approximation (NIBA) by Leggett et al.[3] cannot be justified in this region for temperatures below the Kondo temperature defined as $T_K = \hbar\Delta_r/k_B$, where $\Delta_r = \Delta(\Delta/\omega_c)^{K/(1-K)}$. In fact, if one equates $C(t) = P(t)$ (which NIBA predicts is true), the NIBA would imply certain unphysical properties of the related Kondo problem, such as a divergence in the susceptibility as $T \to 0$.

Furthermore, this parameter region is also interesting in the context of macroscopic quantum coherence, since there could be remnants of coherent (oscillatory) behavior in the zero-temperature dynamics for $1/2 < K < 1$. For this region, NIBA predicts a complete destruction of

quantum coherence. We have studied $P(t)$ at zero temperature in order to check this prediction.

Some numerical results for this parameter region have already been given in Refs. 14 and 15, and a biexponential behavior has been found. However, due to the limitations of our earlier techniques, these simulations were restricted to very small values for the cutoff ($\omega_c/\Delta = 1.25$ has been used in Ref. 15). Furthermore, our previous algorithm did not allow for a study of extremely low temperatures, and we have considered temperatures only slightly below T_K. These shortcomings can be overcome by the algorithm discussed in Sec. II, and we are now able to reach both the scaling region $\omega_c/\Delta \gg 1$ and the zero-temperature limit for $P(t)$. At zero temperature, the time scale of the dynamics should be set solely by the frequency[33]

$$\Delta_{\text{eff}} = [\cos(\pi K)\,\Gamma(1 - 2K)]^{1/2(1-K)}\,\Delta_r\ , \qquad (3.3)$$

where $\Gamma(x)$ denotes the γ function. This effective frequency scale is equal to Δ at $K = 0$, becomes equal to $\pi\Delta^2/2\omega_c$ for $K = 1/2$, and shrinks to zero as $K \to 1$. Since the cutoff ω_c should enter the dynamics only via a renormalization of this effective frequency scale, we use the dimensionless time $y = \Delta_{\text{eff}}t$; at zero temperature, the only system parameter left is the Kondo parameter. As shown by Grabert and Weiss,[33] the NIBA solution for $T = 0$ and $K < 1$ can be written in terms of the Mittag-Leffler function,[34]

$$P_{\text{NIBA}}(y) = E_{2(1-K)}(-y^{2(1-K)})\ . \qquad (3.4)$$

In the parameter region $1/2 \leq K < 1$, this describes a purely incoherent relaxation.

Before discussing the zero-temperature limit for $P(y)$ and $1/2 < K < 1$, we first present data for the correlation function $C(t)$ at $K = 1/2$. This special case has been solved exactly by Sassetti and Weiss,[35] and one finds for sufficiently low temperatures that $C(t)$ approaches zero *from below* at long times. This is reproduced by our simulations shown in Fig. 5; the cutoff chosen here ($\omega_c = 6\Delta$) is already large enough to ensure the validity of $\omega_c/\Delta \gg 1$. Note that the corresponding exact solution for a factorizing initial state, $P(t) = \exp(-\Delta_{\text{eff}}t)$, does not exhibit this behavior.

Finally, in Fig. 6 we show QMC results for the exact $T = 0$ dynamics of $P(y)$ in the Kondo region $1/2 < K < 1$. The cutoff chosen here is within the scaling region $\omega_c/\Delta \gg 1$ so that the dynamics should depend only on the effective time scale $y = \Delta_{\text{eff}}t$. Indeed, as long as $\omega_c/\Delta \geq 5$, we found that a change in the cutoff enters the dynamics solely via Eq. (3.3). Since the frequency Δ_{eff} becomes extremely small with increasing K, it is not possible to numerically study the $T = 0$ dynamics on time scales of the order Δ_{eff}^{-1} for K larger than ≈ 0.75. Here, we have restricted ourselves to $K = 0.6$ and $K = 0.7$, see Fig. 6. For $K = 0.5$, the QMC data for $P(t)$ coincide with the exact solution.

It is not possible to fit the numerical data in Fig. 6 to simple (exponential, biexponential, algebraic, etc.) decay laws. However, it is obvious that *the NIBA gives the correct qualitative picture*, especially at short times.
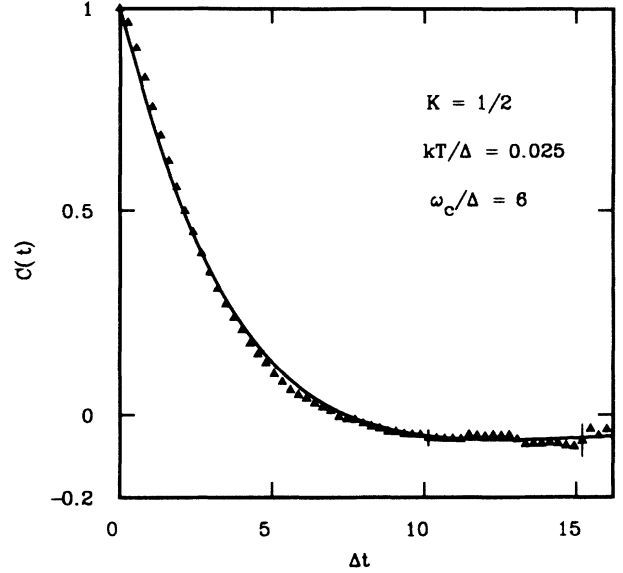

FIG. 5. Symmetrized correlation function $C(t)$ for $K = 1/2$, $\omega_c/\Delta = 6$, and $k_B T/\hbar\Delta = 0.025$. The triangles denote the QMC data for discretization numbers $q = 60$ and $r = 130$. The solid curve is the exact solution from Ref. 35, and vertical bars are error estimates.
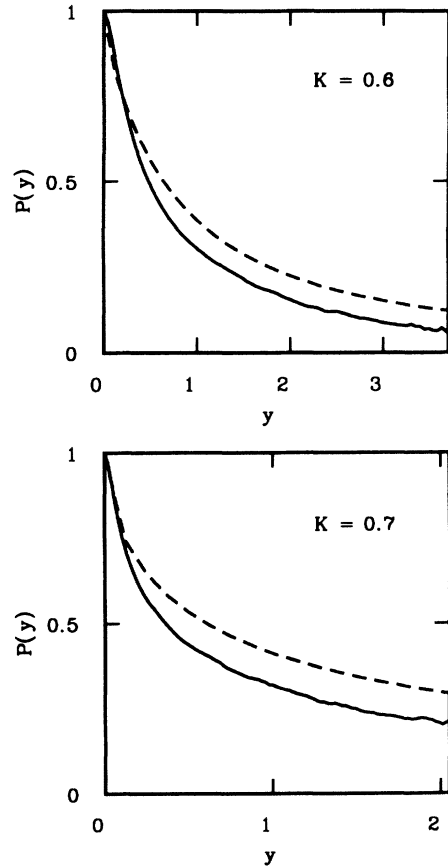

FIG. 6. Zero-temperature dynamics of $P(y = \Delta_{\text{eff}}t)$ in the antiferromagnetic Kondo region. The solid curves are numerically exact results, dashed curves are NIBA predictions. Note the change in effective time scale between both plots. The discretization numbers were $q = 80$ and $q = 160$ for $K = 0.6$ and $K = 0.7$, respectively.

The exact dynamics is fully *incoherent*, yet of quite complicated appearance. These results again underline our earlier finding[13,15] that *the NIBA provides an excellent estimate for P(t) in the bulk of parameter space*. The data shown in Fig. 6 suggest that the NIBA is more accurate for $K = 0.6$; this indicates that the NIBA becomes exact for $P(t)$ as $K \to 1/2$.

One may question how much the respective correlation functions $C(t)$ will deviate from the $P(t)$ depicted in Fig. 6, since $C(t)$ is the relevant quantity for a comparison with the Kondo problem. While the NIBA was shown to give an excellent approximation for the function $P(t)$ even in the low-temperature Kondo region, the quality of the NIBA-prediction $C(t) = P(t)$ seems to be poor in this region (see Fig. 5). We have carried out simulations for $C(t)$ at temperatures slightly below T_K for $1/2 < K < 1$ as well, and the characteristic behavior shown in Fig. 5, namely $C(t)$ approaching zero from below as $t \to \infty$, was found to persist. This would resolve the divergence of the static spin susceptibility[1,35] predicted by NIBA based on $P(t)$ because $P(t)$ and $C(t)$ show qualitatively different behaviors. Such a behavior of $C(t)$ is also in correspondence with the exact Shiba relation.[36]

Unfortunately, we were not able to reach the true zero-temperature limit for the equilibrium correlation function $C(t)$. Clearly, using the same Kadanoff-Baym contour employed in our method would require an infinitely long imaginary-time path for $T = 0$, which makes the algorithm impracticable. By invoking ergodicity arguments,[1] however, a viable variant of our algorithm may facilitate such a calculation. To that purpose, one might consider a factorized initial state at $t_0 < 0$, so that for $t_0 \to -\infty$ the system will be equilibrated at $t = 0$. In effect, one is then left with a real-time contour instead of the Kadanoff-Baym contour, and the initial correlations are represented by negative-time paths. This method is currently under study.

IV. CONCLUSIONS

We have proposed a real-time quantum Monte Carlo simulation method for a numerically exact computation of the dynamical quantities of the spin-boson model. Our technique is based on a discretized path-integral formulation and makes use of the symmetry properties of the dissipative influence functional, whereby one can integrate out the quasiclassical paths and is left with a stochastic sampling of the quantum fluctuations alone. This leads to a significant improvement compared to earlier methods, and allows us to study the dynamics at considerably longer times. The method is generally applicable to dissipative tight-binding systems with arbitrary spectral density.

Results have been presented for two problems of current interest. (a) We have computed the electron-transfer rate constant as a function of the electronic coupling in both the high-temperature and the low-temperature limit. In the high-temperature limit, the classical Marcus result is reproduced; for low temperatures, however, one obtains an oscillatory behavior for large electronic couplings which does not allow for a simple rate description. (b) The dynamics in the antiferromagnetic Kondo region has been computed at $T = 0$ for several values of the Kondo parameter. In accordance with the NIBA, we find a fully incoherent (yet nonexponential) decay for the occupation probability $P(t)$. Initial preparation effects, however, lead to important deviations from the NIBA prediction $C(t) = P(t)$ for the equilibrium correlation function. It is exactly this NIBA equality that led to unphysical results for the equivalent Kondo problem.

ACKNOWLEDGMENTS

* Present address: Fakultät für Physik, Universität Freiburg, Hermann-Herder-Str. 3, D-79104 Freiburg, Germany.

[1] U. Weiss, *Quantum Dissipative Systems*, Series in Modern Condensed Matter Physics Vol. 2 (World Scientific, Singapore, 1993), and references therein.

[2] A.O. Caldeira and A.J. Leggett, Phys. Rev. Lett. **46**, 211 (1981); Ann. Phys. (N.Y.) **149**, 374 (1983); **153**, 445(E) (1983).

[3] A.J. Leggett, S. Chakravarty, A.T. Dorsey, M.P.A. Fisher, A. Garg, and W. Zwerger, Rev. Mod. Phys. **59**, 1 (1987).

[4] U. Weiss, H. Grabert, and S. Linkwitz, J. Low Temp. Phys. **68**, 213 (1987).

[5] H. Wipf, D. Steinbinder, K. Neumaier, P. Gutsmiedl, A. Magerl, and A.J. Dianoux, Europhys. Lett. **4**, 1379 (1987).

[6] J. Kondo, Prog. Theor. Phys. **32**, 37 (1964); A.M. Tsvelick and P.B. Wiegmann, Adv. Phys. **32**, 453 (1983).

[7] For a review, see R.A. Marcus and N. Sutin, Biochim. Biophys. Acta **811**, 265 (1985), and references therein.

[8] J. Ulstrup, *Charge Transfer Processes in Condensed Media* (Springer, New York, 1979).

[9] D. Chandler, in *Liquids, Freezing, and the Glass Transition*, Les Houches Lectures, edited by D. Levesque, J. P. Hansen, and J. Zinn-Justin (Elsevier Science, North-Holland, 1991).

[10] We do not explicitly consider the problem of a particle in an extended double-well potential here. At low enough

temperatures (and under certain restrictions regarding the system parameters) the extended problem reduces to the two-state situation discussed here, see, e.g., A.T. Dorsey, M.P.A. Fisher, and M.S. Wartak, Phys. Rev. A **33**, 1117 (1986).

[11] R.P. Feynman and F.L. Vernon, Ann. Phys. (N.Y.) **24**, 18 (1963).

[12] D. Chandler and P.G. Wolynes, J. Chem. Phys. **74**, 4078 (1981).

[13] C.H. Mak and D. Chandler, Phys. Rev. A **41**, 5709 (1990); **44**, 2352 (1991).

[14] C.H. Mak, Phys. Rev. Lett. **68**, 899 (1992).

[15] R. Egger and U. Weiss, Z. Phys. B **89**, 97 (1992).

[16] C.H. Mak and J.N. Gehlen, Chem. Phys. Lett. **206**, 130 (1993); R. Egger and C.H. Mak, J. Chem. Phys. **99**, 2541 (1993).

[17] V.S. Filinov, Nucl. Phys. B **271**, 717 (1986).

[18] See, for example, J.D. Doll and D.L. Freeman, in *Lasers, Molecules and Methods*, edited by J.O. Hirschfelder, R.E. Wyatt, and R.D. Coalson, Advanced Chemical Physics Vol. LXXIII (Wiley, New York, 1989).

[19] N. Makri, Chem. Phys. Lett. **193**, 435 (1992); M. Topalar and N. Makri, J. Chem. Phys. **97**, 9001 (1992); Chem. Phys. Lett. **210**, 285 (1993); **210**, 448 (1993); D. E. Makarov and N. Makri, Phys. Rev. A **48**, 3626 (1993).

[20] J.E. Gubernatis, M. Jarrell, R.N. Silver, and D.S. Sivia, Phys. Rev. B **44**, 6011 (1991).

[21] R.E. Cline, Jr. and P.G. Wolynes, J. Chem. Phys. **88**, 4334 (1987).

[22] B.A. Mason and K. Hess, Phys. Rev. B **39**, 5051 (1989).

[23] E.Y. Loh, J.E. Gubernatis, R.T. Scalettar, S.R. White, D.J. Scalapino, and R.L. Sugar, Phys. Rev. B **41**, 9301 (1990).

[24] R. Egger and C.H. Mak, J. Phys. Chem. (to be published).

[25] C.H. Mak and R. Egger, Phys. Rev. E **49**, 1997 (1994).

[26] R. Egger, C.H. Mak, and U. Weiss, J. Chem. Phys. **100**, 2651 (1994).

[27] H. Grabert, P. Schramm, and G.-L. Ingold, Phys. Rep. **168**, 115 (1988).

[28] A. Schmid, J. Low Temp. Phys. **49**, 609 (1982).

[29] The last term in the influence functional (2.19) modifies only the matrix $\mathbf{V}^{(1)}$. Note that the path combinatorics is already contained in the definition of the $\mathbf{V}^{(j)}$ matrices, since some of these matrix elements are zero. Finally, for a general tight-binding system with d states, we have to deal with a matrix multiplication of q $(2d+1 \times 2d+1)$ matrices.

[30] J.P. Valleau and S.G. Whittington, in *Statistical Mechanics, Part A: Equilibrium Techniques*, edited by B.J. Berne, Modern Theoretical Chemistry Vol. 5 (Plenum, New York, 1977).

[31] A. Garg, J.N. Onuchic, and V. Ambegaokar, J. Chem. Phys. **83**, 4491 (1985).

[32] S.S. Skourtis, A.J.R. da Silva, W. Bialek, and J.N. Onuchic, J. Phys. Chem. **96**, 8034 (1992).

[33] H. Grabert and U. Weiss, Phys. Rev. Lett. **54**, 1605 (1985).

[34] A. Erdelyi, *Higher Transcendental Functions* (McGraw-Hill, New York, 1955), Vol. 3.

[35] M. Sassetti and U. Weiss, Phys. Rev. A **41**, 5383 (1990).

[36] H. Shiba, Prog. Theor. Phys. **54**, 967 (1975).